*Article*

# Temperature Modeling with the Group Method of Data Handling to Inform Projected Rainfall Depth Changes for Extreme Events in Central West, New South Wales, Australia

Ronald William Lake [1], Saeed Shaeri [1,2,]* and S. T. M. L. D. Senevirathna [1,2]

[1]   School of Computing, Mathematics and Engineering, Charles Sturt University, Bathurst, NSW 2795, Australia
[2]   Gulbali Institute, Charles Sturt University, Bathurst, NSW 2795, Australia
*   Correspondence: sshaeri@csu.edu.au; Tel.: +61-2-633-82619

**Abstract:** The focus of this research is to introduce the application of the polynomial neural network of the group method of data handling (GMDH) for the first time in the regional area of the New South Wales state of Australia. Within this regional context, temperature data are modeled to assess its projected variation impacts on rainfall depth due to climate change. The study area encompasses six local government areas within the state's Central West region. Stochastic methods for monotonic trend identification were used to support the modeling. Four established homogeneity tests were also used for assessing data integrity by determining the frequency of breakpoints within the mean of the data. The results of the GMDH modeling returned a coefficient of determination exceeding 0.9 for all stations dominated by an overall upward trend with an average maximum temperature increase of 0.459 °C per decade across the study region. The homogeneity tests found all data categorized as useful within the context of applicability for further climate change studies. By combining the modeled upward temperature trend with the intensity frequency distribution (IFD) design rainfall modification factor, projected depth increases by 2070 are obtained, enabling improved designs for stormwater infrastructure based on classified temperature variation scenarios.

**Keywords:** GMDH; temperature trend; climate change; homogeneity tests

## 1. Introduction and Background

Climate change effects are neither uniformly nor universally distributed around the world. There are notable distinctions between regions within countries and also between hemispheres. Furthermore, it is frequently ascertained that in the future, more intense rainfall and peak flows are anticipated in urban areas. Likewise, rainfall across Australia is subject to extreme variability due largely to the diversity of the topography, geomorphology, and proximity to the coast. Such a rainfall increase will have a performance impact on conventional urban drainage systems with more voluminous flows, rainfall events of increasing duration, and more frequent pluvial flooding. However, factors, such as location and season, impact rainfall patterns with much greater noticeability than it does the temperature, which, by itself, on average has risen across much of Australia since 1960. Hence, quantifying Australia's average annual rainfall has much less meaning than referring to Australia's average annual temperature [1].

As shown by many researchers, the authors of [2–11] found both temperature and rainfall changes to be highly characteristic of climate change. Meanwhile, urban developments both within cities and rural areas have contributed to the undesirable effects of large floods, mostly due to the increasing percentage of impervious surfaces and the volumetric increase in runoff that results, making the effects of climate change markedly more significant [3,4,9,12]. However, it is onerous to simultaneously simulate temperature and precipitation variabilities, owing to the correlation between them [2,3,7,10]. Therefore, the dominant focus by most researchers tends to be placed on either one of the parameters

whilst correlating the climate change impact [5,7,9,11]. Accordingly, this study aimed at establishing a relationship between publicly available air temperature data, projected over 50 years, and extreme rainfall events in 2070, instead of simultaneously having both parameters as input to a predictive model.

In a study undertaken by Karl et al. [13], detailing the prior 50 years, the volume of rainfall from the most significant 1% annual exceedance probability (AEP) events increased by 20% in the USA southeast. This illustrates the change in rainfall volume initiated by climate change that could be observed in other places as well. Increased rainfall intensity commensurate with an increase in the surface area percentage of impervious surfaces will "cause flashier runoff periods", peak flows of greater magnitude, and an increased probability of flooding [14]. The authors of [15] (p. 290) also detail how climate change-induced rainfall intensity increases are a significant "threat to infrastructure systems, especially stormwater infrastructure systems, and the transportation systems that they protect". The overwhelming assumption by the authors in [15] is that stormwater systems throughout the world have been and continue to be designed on the premise of a stationary climate. With the effects of climate change, however, this philosophy can no longer be applied with any degree of reliability. Meanwhile, trend analysis has been used with success (e.g., [2,4–11,16–19]) to track long-term changes over periods of study as indicative of climate change. In modeling temperature data, as a means of illustrating the correlation with rainfall, the connection is reinforced through the work of Westra et al. [20] showing that the intensity of extreme hourly or sub-hourly rainfall is sensitive to local atmospheric temperatures. Moreover, the studies by Huang et al. [21] find an increase in extreme rainfall intensity of 7%/°C due to increasing atmospheric temperatures.

Meanwhile, the report produced by the IPCC in 2022 [22] states an increase in drought frequency and extreme fires in southern and eastern Australia is projected with high confidence. Rainfall data, though, have been contradictory across the past three decades, indicating both increasing and/or decreasing trends across different regions within Australia [22]. However, largely, the degree of confidence in temperature variations due to climate change is seen by the Australian rainfall and runoff (ARR) project with greater reliability than for changes in rainfall patterns [23].

To cater to the variability in rainfall whilst providing a linkage with warming temperatures, ARR provides an adjustment factor for intensity–frequency–distribution (IFD) curves that are only functions of projected temperature changes [23]. The temperature projections are subsequently combined with changes to "extreme rainfall event intensities" framed by existing research both in Australia and overseas. Data on the water holding capacity of a warmer atmosphere, assessments based upon observations, and experimental data from high-resolution dynamic downscaling in combination suggest an expected change in the intensity of heavy rainfall to be within the range of 2% to 15%/°C of temperature increase in Australia [23]. Hence, due to the significant variability in regional rainfall, and the uncertainty in rainfall projections, an increase in either intensity or depth of 5%/°C of local warming is advised by ARR [23] (Book 1) as seen in Equation (1) below.

Using the projected increase in temperature to predict the increase in extreme rainfall intensity, ARR provides a means of calculating such an increase, which is termed "the midpoint approach":

$$I_p = (I_{ARR})1.05^{T_m} \tag{1}$$

In this equation, $I_p$ is the projected increase in rainfall intensity or depth (in mm), $I_{ARR}$ is the design rainfall depth for the current conditions (extracted in this research from the data available on the Australian Bureau of Meteorology (BoM) website [24]), and $T_m$ is the median temperature within the class interval of temperature increase (as explained by [23], Book 1, page 165). That is, for the class intervals of 1.5 to 3 °C 'hotter' global temperature compared to baseline temperature, the median temperature would be $(1.5 + 3)/2 = 2.25$ °C. This moderated increase (i.e., using the median temperature) is a result of the degree of applicability across all frequencies and durations, as there is no guarantee that static scaling can be applied equally. "Regional atmospheric circulation, synoptic systems, and

soil wetness" [23] (Book 1, p. 161) are other factors that can potentially affect the future intensity of precipitation or depth over land. However, in order to make the assumption about the 2.25 °C median temperature increase, the researcher should satisfy themselves if such an assumption is valid at their desired location. Accordingly, one approach would be the use of climate models, which are traditionally used to forecast weather conditions but require a large and complicated historical input dataset. The other approach, which has gained popularity, utilizes statistical simulations, such as linear time-series models (LTS), autoregressive integrated moving average models (ARIMA), or artificial neural networks (ANN), which are computationally significantly cheaper than forecasting models. ANNs methods are data-driven, trained, corrected, and adjusted mostly automatically and are flexible in terms of climate data. Accordingly, to analyze the existing temperature data, in this research, we use the group method of data handling (GMDH) to project the temperature variations and partially test the applicability of the projected figures.

GMDH is a machine learning approach, implemented as a polynomial neural network and an inductive learning paradigm based on the Kolmogorov–Gabor polynomial equations, trained through the process of supervised learning [25]. This learning process seeks to find relationships that exist between the time series data, construct forecasting models automatically, and enable the system algorithm to predict future outcomes based on current data [25]. The GMDH algorithm is particularly suited to analyzing time series nonlinear datasets, such as weather modeling, and its forecasting capability is extremely important in the light of climate change, particularly in terms of runoff and stormwater infrastructure. The supervised learning approach of GMDH selects a random subset of 30% of the data for training the model. The GMDH machine learning algorithm then produces a model from which the trend is identified. This outcome is achieved by modeling the full extent of input variable combinations and then selecting the optimum model that has been produced from the full range of models according to the external criterion. That is, the optimum solution is specified by the external criterion by presenting models exhibiting equivalent degrees of complexity. The chosen model will deliver a minimum value within the plane of complexity, and it is this model that GMDH uses to present the temperature trend [26].

In this study, to complement the GMDH modeling, two stochastic monotonic trend depiction methods are also utilized given the recorded temperature data are independent. The first one is the Mann–Kendall (MK) trend test [9,27,28], which is a non-parametric test with low sensitivity to discontinuities that present within an inhomogeneous time series or any outliers that could be found in the skewed hydrometeorological dataset [7,9,17]. The strength of the identified trend is described by the magnitude of the MK test parameter Z (which is not described here for the sake of brevity). The MK test assesses the null hypothesis ($H_0$) at a specific significant level (e.g., 5% or 1%) on the assumption that no monotonic trend exists within the data, whilst the alternative hypothesis ($H_a$) assumes the position that there is a monotonic trend within the data [9,18]. Applying the MK test is important to ensure the available temperature data are monotonic, and consistently increasing or decreasing over time, to then justify that projection over 50 years ahead is plausible [19,29]. The second stochastic method, which typically accompanies the MK test, is Sen's slope estimate (SSE), which is a non-parametric process for ascertaining the slope of a trend within a set of data pairs [9,29,30]. The numeric results of this test indicate whether there is a positive slope (or trend) for the temperature as we know it, or whether the dataset processing attempt signals it otherwise. Both of these tests are considered non-parametric, meaning that there is no need to assume a distribution model (such as a normal distribution) for data processing [9]. Additionally, four established homogeneity tests for data integrity are utilized here, providing guidance and assurance on possible change points within the data that could be related to exogenous non-climate-related events [31]. The four tests encompass the non-parametric Pettitt test (PT), the parametric standard normal homogeneity test (SNHT), the parametric Buishand range test (BR), and the non-parametric von Neumann test (VNR) [8,31–34].

Other approaches that are used by other researchers for trend analysis or forecast of temperature and rainfall data mostly include more sophisticated processes. For example, the authors of [4] took a seemingly simpler approach by utilizing the climate moisture index (CMI), analysis of variance (ANOVA), and regression analysis of overtime data to find long-term trends. The authors of [9], combined MK and SSE with an innovative trend analysis (ITA) method, but conclude that the "ITA method is more complex". They chose to divide the rainfall data into three categories (low, middle, and high) but later explained that "even though ITA has the advantage of estimating hidden trends at three categories of the data point, in this study, it was found that defining the boundary of low, middle, and high data values is not as simple" [9]. Similarly, the authors of [3] used a modified version of the MK test, along with SSE and ITA, but stated that their analyses showed different behavior with different tests. Similar issues inspired the authors of [5] to apply the innovative triangular trend analysis (ITTA) methodology instead "for its effectiveness and success for partial trend component identification". As ITTA "is based on dividing the time series into subintervals (series) of equal length and comparing each, pairwise", in combination with an "orthogonal Discrete Wavelet Transform (DWT) for partial trend identification", they were able to show "a good efficiency for extreme rainfall event detection [5]." Furthermore, the authors of [7] combined the MK test with "the quantile regression (QR) methods to provide a more comprehensive picture of extreme precipitation events", investigating "the temporal trend in different quantiles of the historical time series". That is, this method provides more insight by looking at previously known separate timeframes. The authors of [10] used long short-term memory (LSTM) neural network method to predict their respective data with "long intervals and time delays in time series". However, they reported that "the main drawback of LSTM processing . . . is that the input one dimensional vector must be expanded before processing. Thus, all spatial information is lost during processing." The authors of [6], introduced the standardized precipitation index (SPI) and standardized precipitation evapotranspiration index (SPEI), along with MK and SSE tests, to characterize the occurrence of drought in European Coastal Metropolitan. Their conclusion is that "the findings from SPEI clearly contrast with those from the SPI series. . . . SPI and SPEI portray differently the direction of changes of drought occurrences . . . [however] SPI is still very useful, especially where temperature data are missing".

Thus, within the extent of this literature review, no one approach could satisfy the requirements of this research and assist the authors to achieve their aim, which is solely to project rainfall depth for 2070 in the study area against the design depth in 2020. However, utilizing GMDH, along with the complementary tests, and simple ARR's projected increase in rainfall intensity equation, do provide the desired outcome as explained below.

## 2. Study Area

This study focuses on the Central West region within the state of New South Wales (NSW), Australia, occupying an area of about 63,000 km$^2$ and covering a total of 13 local government areas (LGAs) according to Regional Development Australia [35]. The topographical heterogeneity of the region identifies some climatic sub-regions that experience distinct weather and climate patterns. Hence, to maximize the degree of geomorphological homogeneity within a climate context, this research focuses on the town of Forbes (33.3845° S, 148.0078° E) within the Forbes LGA (Figure 1), and its surrounding LGAs of Parkes, Lachlan, Bland, Weddin, and Cowra (Table 1).
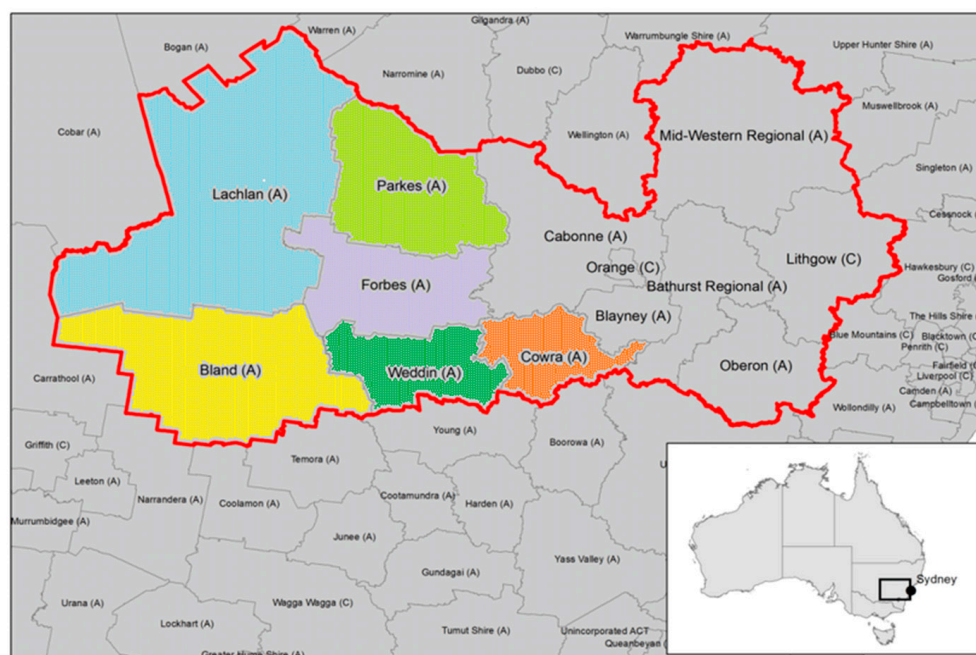
**Figure 1.** Australia's NSW Central West region (Reprinted/adapted with permission from Ref. [36]. 2015, APCBSS).

**Table 1.** Details of the study stations.

| Station Location | LGA | Commenced Recording Data | Site Number | Latitude (°S) | Longitude (°E) | Elevation (m) |
|---|---|---|---|---|---|---|
| Condobolin Ag Research St | Lachlan | 1954 | 50052 | 33.07 | 147.23 | 195 |
| Condobolin Airport | Lachlan | 1993 | 50137 | 33.07 | 147.21 | 193 |
| Cowra Airport | Cowra | 2004 | 65111 | 33.84 | 148.65 | 300 |
| Forbes Airport | Forbes | 1966 | 65103 | 33.36 | 147.92 | 230 |
| Grenfell Manganese Road | Weddin | 1995 | 73014 | 33.89 | 148.15 | 390 |
| Lake Cargelligo Airport | Lachlan | 1885 | 75039 | 33.28 | 146.37 | 169 |
| Parkes Airport | Parkes | 1881 | 65068 | 33.13 | 148.24 | 323 |
| Peak Hill Post Office | Parkes | 1941 | 50031 | 32.72 | 148.19 | 285 |
| West Wyalong Airport | Bland | 1890 | 50017 | 33.94 | 147.20 | 257 |
| Wyalong Post Office | Bland | 1999 | 73054 | 33.93 | 147.24 | 245 |

Figure 2 depicts the variation of the mean monthly maximum temperature (°C) and mean monthly rainfall depth (mm) over the entire records at each of the selected 10 stations in this research (Table 1). As seen, temperature variation is very similar between various locations; however, rainfall depth does not show any consistency or trend over the years even though there are geographic/topographic similarities between the stations. Figure 2 also reveals that establishing a unique trend or a two-input model would not provide a justifiable opportunity to make forecasts at a desirable time in the future, requiring the establishment of more sophisticated climate models or alike to achieve an acceptable outcome.
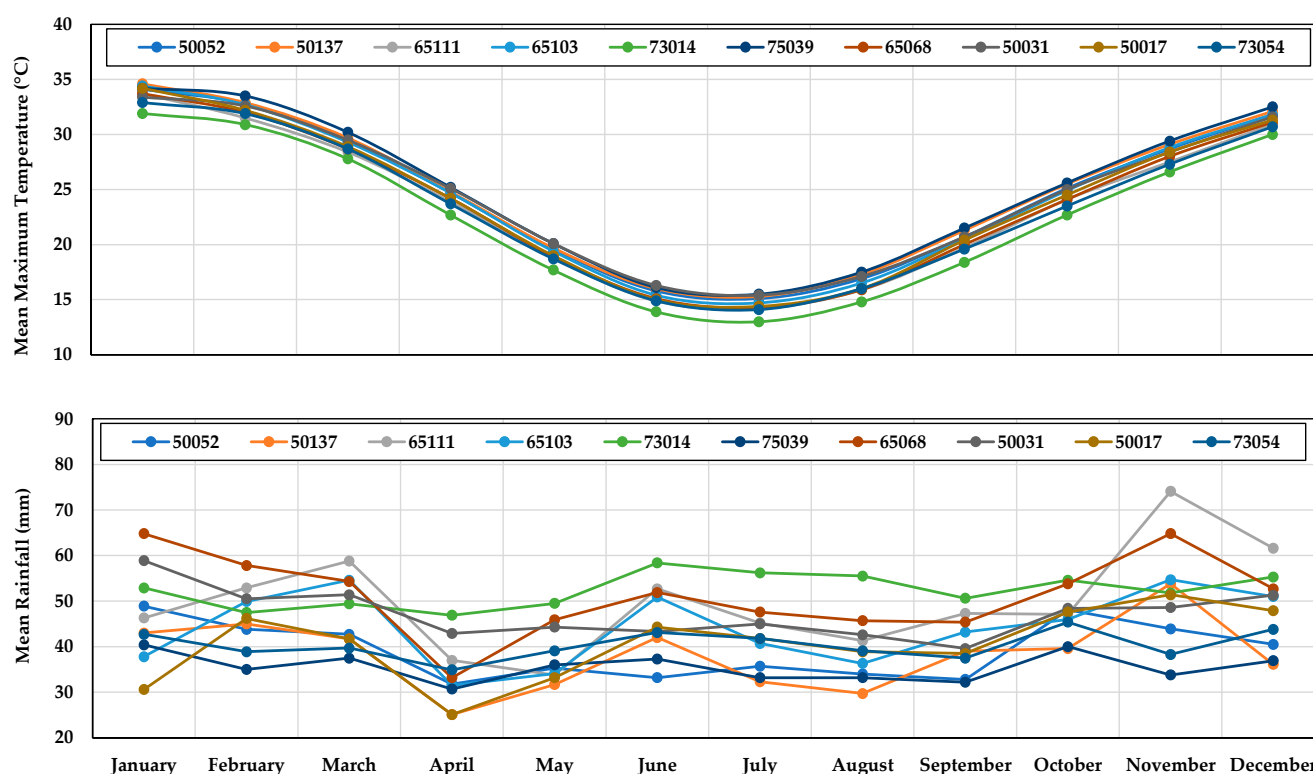
**Figure 2.** Mean monthly maximum temperature (°C) and rainfall depth (mm) variations for various stations (check Table 1 for the station names).

### 3. Materials and Methods

Available daily temperature data on the Australian Bureau of Meteorology (BoM) website [37] from the 10 stations in the study area (Table 1) are first downloaded from the first available record until 2020. As seen in Table 1, available data spans distinct timeframes, ranging from 16 to 139 years, with minor discontinuities. Temperature data are analyzed as distinct entities within each LGA, thereby providing the potential for comparative analyses with adjoining stations/LGAs. That is, there is no need to combine the data from two different locations to establish a larger database. Instead, it is important to compare different locations to enable the provision of spatial outcomes for greater usage within various contexts. The logic behind this approach is that different timelines have the potential to present trends that may be quite distinct (as seen in Figure 2), which may potentially lead to skewed datasets if two timelines are convolved to deliver a third. Moreover, variations in the range of the data vary not just within a single station but also across all LGAs, as depicted in Figure 2.

No attempt was made to fill in any gaps in the data, as GMDH can deal with gaps; nevertheless, for temperature modeling, the need to implement short-time lags is not necessary as there are minimal deviations in proximal readings. Having data available, then, GMDH Shell version 3.0 [38] is utilized for data processing by directly importing temperature data as a CSV file for each station. This allows GMDH to provide trends of the mean maximum temperature increase (°C/year). At this stage, the coefficient of determination ($R^2$) is used to ensure success in GMDH modeling. The control of $R^2$ is deemed sufficient, as there are other ways in this study to control the existing and projected data. That is, as described earlier, the two stochastic trend depiction methods of MK and SSE are used to complement GMDH modeling and ensure consistency between various outcomes.

Finally, the software XLSTAT by Addinsoft [39], which is a statistical add-in for Microsoft Excel, is utilized for trend and homogeneity testing, i.e., determination of MK, SSE, PT, SNHT, BR, and VNR results, on the actual data (but not the modeled GMDH

data). The process requires selecting the station CSV file and choosing the required trend or homogeneity test for data assessment within XLSTAT.

## 4. Results

For each of the selected weather stations within the study area, the provided mean maximum monthly temperature data are processed first. As seen in Table 2, the coefficient of determination ($R^2$) provides a comparative analysis between the actual and modeled data by GMDH in support of the modeling accuracy; that is, all figures are close to one. Accordingly, this strongly indicates that our GMDH model fits the non-parametric dataset with a high degree of precision with all $R^2$ values exceeding 0.9. Moreover, a positive increasing temperature trend across the study area is observed by both GMDH and SSE methods (Table 2), ranging from 0.024 to 0.084 °C/year. This illustrates an average 0.459 °C and 0.501 °C increase in temperature per decade, respectively for GMDH and SSE methods. By comparison, a study by Wang et al. [40], mapping across the area of this study, using 19 global climate models, projected a mean maximum decadal increase ranging from 0.07 °C to 0.45 °C from 2020 to 2100.

**Table 2.** Trends of the mean maximum temperature increase (°C/year), using SSE and GMDH methods along with the coefficients of determination ($R^2$) for the success in GMDH modeling.

| Station Location | Site Number | SSE | GMDH | $R^2$ |
|---|---|---|---|---|
| Condobolin Ag Research St | 50052 | 0.036 | 0.026 | 0.921 |
| Condobolin Airport | 50137 | 0.076 | 0.084 | 0.916 |
| Cowra Airport | 65111 | 0.050 | 0.059 | 0.951 |
| Forbes Airport | 65103 | 0.050 | 0.042 | 0.941 |
| Grenfell Manganese Road | 73014 | 0.031 | 0.025 | 0.928 |
| Lake Cargelligo Airport | 75039 | 0.055 | 0.053 | 0.923 |
| Parkes Airport | 65068 | 0.046 | 0.040 | 0.917 |
| Peak Hill Post Office | 50031 | 0.046 | 0.038 | 0.919 |
| West Wyalong Airport | 50017 | 0.069 | 0.068 | 0.930 |
| Wyalong Post Office | 73054 | 0.042 | 0.024 | 0.957 |

Furthermore, in our analysis, the homogeneity tests found the frequency of breakpoints within the mean of each dataset to be at most one, allowing all to be categorized as useful. Likewise, the MK trend test (not shown here) returned in favor of a monotonic positive temperature trend at Peak Hill, but at no other station. These two results imply that the dataset can be used reliably for further climate studies and projections into the future, as discussed further below.

From the GMDH modeling data above, the predicted mean maximum temperature increase, based upon linear extrapolation, correlates to an increase of 2.286 °C by 2070, averaged across the chosen 10 stations. It is worth noting that the NSW Office of the Environment and Heritage [41] also details a class interval of 1.5 to 3.0 °C for the same period over the Central West of NSW, which provides the boundaries for the ARR's midpoint approach of 2.25 °C [23]. Substituting 1.5, 2.25, and 3.0 °C increases in Equation (1) and using the 2020 design rainfall depth (in mm) extracted from BoM [37], the rainfall depth for 2070 can be found across the study area for a 60-min 1% AEP event against the design depth in 2020. This result is shown graphically in Figure 3. The LGAs are sorted based on their predicted design rainfall depth (in mm) in 2070.
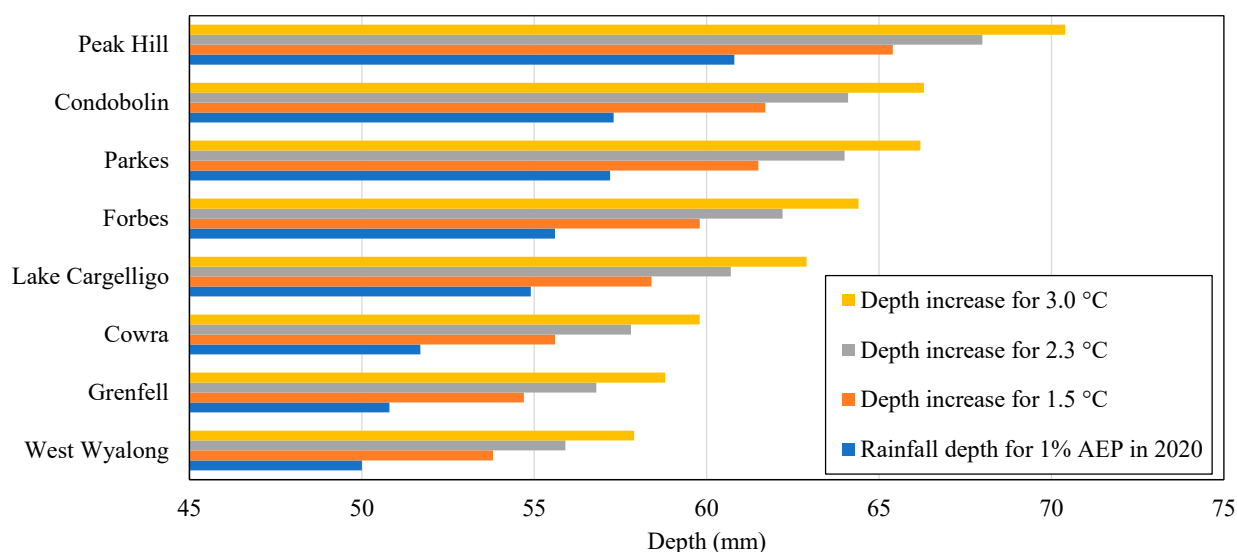
**Figure 3.** The 2070 projections compared with the current rainfall depth for a 60 min event of 1% AEP.

## 5. Discussion

As stated above, GMDH and the analysis using SSE all produce aligning positive trends (Table 2), their distinction being the former is based upon the model, and the latter on the BoM actual data. With supportive trends, the capacity to predict a mean maximum temperature increase of 2.286 °C by 2070 across the study area is realized. The MK test found a statistically significant temperature trend for Peak Hill but not for other stations. The implication is that at a 95% confidence interval, there was a significant monotonic trend detected within the data but only for Peak Hill. The MK test though does not identify the trend as being linear or non-linear [42]. However, these results align with the Western Enabling Regional Adaption: Central West and Orana Region Report findings [41]. That is, the projected temperature increase is based upon linear interpolation of the positive trend, which is reflected within the temperature data.

The conservative increase in rainfall depth, as illustrated in Figure 3, ranges from 3.8 mm at West Wyalong for a 1.5 °C increase to 9.6 mm at Peak Hill for a 3.0 °C increase by 2070. With extreme rainfall events commencing with the 1% AEP, the duration can range from 1-min through to 3-h for applications to civil engineering works. However, this study concentrated on the 60-min event, so events of other durations may deliver projected outcomes that change the order of depth increase from those presented in Figure 3. The approach presented within [23], and accordingly the outcome of this study for extreme rainfall projections is, however, conservative. Nevertheless, the results presented for the determination of extreme rainfall depth increases using Equation (1) reflect that approach, the inference being that the actual figures for depth increases could potentially be more extreme.

The opportunity that exists to adopt this approach can be used to inform future planning, design, and management of stormwater infrastructure across the study area. By catering to an increase in extreme rainfall intensity, planners can be better placed to provide containment measures for pluvial flooding within their designs.

## 6. Conclusions

This research study aimed to add to the existing body of knowledge through the examination of monthly maximum temperature data obtained from a publicly available domain (i.e., the Australian Bureau of Meteorology (BoM) website) for trend analysis identification through the group method of data handling (GMDH) modeling and future projection due to climate change. Accordingly, the Australian rainfall and runoff (ARR) adjustment factors for intensity–frequency–distribution (IFD) curves are utilized to link the

projected temperature increase to rainfall intensity. However, to ensure the applicability of this methodology, the results of the GMDH modeling and trend analysis are cross-controlled using the Mann–Kendall trend test, Sen's slope estimate method, and four homogeneity tests (i.e., Pettitt's, standard normal homogeneity, Buishand's range, and von Neumann's ratio tests). Those results are all found conclusive in analyzing data integrity, producing supportive temperature trends, and allowing the projection to be done for an increase in temperature from 2020 to 2070 across the study area. Hence, the success of this research indicates that the opportunity exists to model temperature data using GMDH, ideally for new knowledge generation over a greater number of stations across a larger area as a means of furthering meteorological insights into the future.

## References

1.  Cleugh, H.; Smith, M.S.; Battaglia, M.; Graham, P. *Climate Change: Science and Solutions for Australia*; CSIRO Publishing: Clayton, Australia, 2011.
2.  Rana, A.; Moradkhani, H.; Qin, Y. Understanding the joint behaviour of temperature and precipitation for climate change impact studies. *Theor. Appl. Climatol.* **2017**, *129*, 321–339. [CrossRef]
3.  Quenum, G.M.; Nkrumah, F.; Klutse, N.A.; Sylla, M.B. Spatiotemporal Changes in Temperature and Precipitation in West Africa. Part I: Analysis with the CMIP6 Historical Dataset. *Water* **2021**, *13*, 3506. [CrossRef]
4.  Shikwambana, S.; Malaza, N.; Shale, K. Impacts of Rainfall and Temperature Changes on Smallholder Agriculture in the Limpopo Province, South Africa. *Water* **2021**, *13*, 2872. [CrossRef]
5.  Zerouali, B.; Al-Ansari, N.; Chettih, M.; Mohamed, M.; Abda, Z.; Santos, C.A.; Zerouali, B.; Elbeltagi, A. An Enhanced Innovative Triangular Trend Analysis of Rainfall Based on a Spectral Approach. *Water* **2021**, *13*, 727. [CrossRef]
6.  Espinosa, L.A.; Portela, M.M.; Matos, J.P.; Gharbia, S. Climate Change Trends in a European Coastal Metropolitan Area: Rainfall, Temperature, and Extreme Events (1864–2021). *Atmosphere* **2022**, *13*, 1995. [CrossRef]
7.  Jamali, M.; Gohari, A.; Motamedi, A.; Haghighi, A.T. Spatiotemporal Changes in Air Temperature and Precipitation Extremes over Iran. *Water* **2022**, *14*, 3465. [CrossRef]
8.  Todaro, V.; D'Oria, M.; Secci, D.; Zanini, A.; Tanda, M.G. Climate Change over the Mediterranean Region: Local Temperature and Precipitation Variations at Five Pilot Sites. *Water* **2022**, *14*, 2499. [CrossRef]
9.  Toni, A.T.; Malcherek, A.; Kassa, A.K. Agroclimatic Zone-Based Analysis of Rainfall Variability and Trends in the Wabi Shebele River Basin, Ethiopia. *Water* **2022**, *14*, 3699. [CrossRef]
10. Wu, S.; Fu, F.; Wang, L.; Yang, M.; Dong, S.; He, Y.; Zhang, Q.; Guo, R. Short-Term Regional Temperature Prediction Based on Deep Spatial and Temporal Networks. *Atmosphere* **2022**, *13*, 1948. [CrossRef]
11. Ahmad, K.; Banerjee, A.; Rashid, W.; Xia, Z.; Karim, S.; Asif, M. Assessment of Long-Term Rainfall Variability and Trends Using Observed and Satellite Data in Central Punjab, Pakistan. *Atmosphere* **2023**, *14*, 60. [CrossRef]
12. Roozbahani, A.; Behzadi, P.; Bavani, A.M. Analysis of performance criteria and sustainability index in urban stormwater systems under the impacts of climate change. *J. Clean. Prod.* **2020**, *271*, 122727. [CrossRef]
13. Karl, T.R.; Melillo, J.M.; Peterson, T.C. *Global Climate Change Impacts in the United States*; Cambridge University Press: Cambridge, MA, USA, 2009.
14. Semadeni-Davies, A.; Hernebring, C.; Svensson, G.; Gustafsson, L.-G. The impacts of climate change and urbanisation on drainage in Helsingborg, Sweden: Suburban stormwater. *J. Hydrol.* **2008**, *350*, 114–125. [CrossRef]
15. Cook, L.M.; McGuinnis, S.; Samaras, C. The effect of modelling choices on updating intensity-duration-frequency curves and stormwater infrastructure designs for climate change. *Clim. Chang.* **2020**, *159*, 289–308. [CrossRef]

16. Safavi, H.R.; Sajjadi, S.M.; Raghibi, V. Assessment of climate change impacts on climate variables using probabilistic ensemble modelling and trend analysis. *Theor. Appl. Climatol.* **2017**, *130*, 635–653. [CrossRef]
17. Wang, F.; Shao, W.; Yu, H.; Kan, G.; He, X.; Zhang, D.; Ren, M.; Wang, G. Re-evaluation of the power of the Mann-Kendall test for detecting monotonic trends in hydrometeorological time series. *Front. Earth Sci.* **2020**, *8*, 14. [CrossRef]
18. Önöz, B.; Bayazit, M. Block Bootstrap for Mann-Kendall Trend Test of Serially Dependent Data. *Hydrol. Process.* **2012**, *26*, 3552–3560. [CrossRef]
19. Mavromatis, T.; Stathis, D. Response of the water balance in Greece to temperature and precipitation trends. *Theor. Appl. Climatol.* **2011**, *104*, 13–24. [CrossRef]
20. Westra, S.; Fowler, H.J.; Evans, J.P.; Alexander, L.V.; Berg, P.; Johnson, F.; Kendon, E.J.; Lenderink, G.; Roberts, N.M. Future changes to the intensity and frequency of short-duration extreme rainfall. *Rev. Geophys.* **2014**, *52*, 522–555. [CrossRef]
21. Huang, J.; Fatichi, S.; Mascaro, G.; Manoli, G.; Peleg, N. Intensification of sub-daily rainfall extremes in a low-rise urban area. *Urban Clim.* **2022**, *42*, 101124. [CrossRef]
22. IPCC. *Climate Change 2022: Impacts, Adaption, and Vulnerability. Intergovernmental Panel on Climate Change—Technical Summary*; IPCC: Geneva, Switzerland, 2022.
23. ARR. Australian Rainfall and Runoff: A Guide to Flood Estimation—Book 1: Scope and Philosophy. Available online: http://www.arr-software.org/pdfs/ARR_190514_Book1.pdf (accessed on 6 May 2020).
24. BoM. Bureau of Meteorology: 2016 IFDs (New). Available online: http://www.bom.gov.au/water/designRainfalls/revised-ifd/ (accessed on 6 May 2020).
25. Dag, O.; Yozgatligil, C. GMDH: An R package for short term forecasting via GMDH-type neural network algorithms. *R J.* **2016**, *8*, 379–386. [CrossRef]
26. Lake, R.W.; Shaeri, S.; Senevirathna, S.T.M.L.D. Review of the Limitations and Potential Empirical Improvements of the Parametric Group Method of Data Handling for Rainfall Modelling. *J. Environ. Sci. Pollut. Res.* **2022**, 1–15. [CrossRef] [PubMed]
27. Mann, H.B. Non-parametric tests against trend. *Econometrica* **1945**, *13*, 245–259. [CrossRef]
28. Kendall, M.G. *Rank Correlation Methods*, 4th ed.; Charles Griffin: London, UK, 1975.
29. Gocic, M.; Trajkovic, S. Analysis of changes in meteorological variables using Mann-Kendall and Sen's slope estimator statistical tests in Serbia. *Glob. Planet. Chang.* **2013**, *100*, 172–182. [CrossRef]
30. Sen, P.K. Estimates of the Regression Coefficient based on Kendall's Tau. *J. Am. Stat. Assoc.* **1968**, *63*, 1379–1389. [CrossRef]
31. Costa, A.C.; Soares, A. Homogenization of climate data: Review and new perspectives using geostatistics. *Math. Geosci.* **2009**, *41*, 291–305. [CrossRef]
32. Kang, H.M.; Yusof, F. Homogeneity Tests on Daily Rainfall Series in Peninsular Malaysia. *Int. J. Contemp. Math. Sci.* **2012**, *7*, 9–22.
33. Javari, M. Trend and Homogeneity Analysis of Precipitation in Iran. *Climate* **2016**, *4*, 44. [CrossRef]
34. Mahmood Agha, O.M.A.; Çağatay Bağçacı, S.; Şarlak, N. Homogeneity Analysis of Precipitation Series in North Iraq. *IOSR J. Appl. Geol. Geophys.* **2017**, *5*, 57–63. [CrossRef]
35. RDA. *Our Region: Central West*; Regional Development Australia: Canberra, Australia, 2020.
36. MacFarlane, J.; Blackwell, B.D.; Mounter, S.W. Good gardening for a perennial economy: What's the optimal growth for a regional economy? In Proceedings of the Asia Pacific Conference on Business and Social Sciences 2015, Kuala Lumpur, Malaysia, 23–24 November 2015.
37. BoM. Bureau of Meteorology: Climate Data Online. Available online: http://www.bom.gov.au/climate/data/ (accessed on 6 May 2020).
38. GMDH. The Best Time Series Analysis Solution in 2021. GMDH Shell Version 3.0. Available online: https://gmdhsoftware.com/time-series-analysis-software (accessed on 10 October 2021).
39. Addinsoft. XLSTAT BASIC: Explore, Visualise and Model Your Data in One Interface. Available online: https://www.xlstat.com/en/solutions/basic/ (accessed on 20 January 2021).
40. Wang, B.; Liu, D.E.; Asseng, S.; Macadam, I.; Yu, Q. Impact of climate change on wheat flowering time in eastern Australia. *Agric. For. Meteorol.* **2015**, *209–210*, 11–21. [CrossRef]
41. OEH. *Western Enabling Regional Adaptation—Central West and Orana Region Report*; NSW Office of the Environment and Heritage: Sydney, Australia, 2017.
42. Jain, S.K.; Kumar, V.; Saharia, M. Analysis of rainfall and temperature trends in northeast India. *Int. J. Climatol.* **2013**, *33*, 968–978. [CrossRef]